



Electrochemical extraction of lead from urea–1-ethyl-3-methylimidazolium fluoride system containing PbO at 353 K

Wen-cai HE^{1,2}, Feng-guo LIU¹, Xiong-wei ZHONG³, Shan YANG², Zhong-ning SHI⁴

1. Key Laboratory for Ecological Metallurgy of Multimetallic Mineral (Ministry of Education),
Northeastern University, Shenyang 110819, China;

2. Department of Chemistry, Physics and Atmospheric Science, Jackson State University, Jackson, MS 39217, USA;

3. Shenzhen Geim Graphene Center, Tsinghua–Berkeley Shenzhen Institute &

Tsinghua Shenzhen International Graduate School, Tsinghua University, Shenzhen 518055, China;

4. State Key Laboratory of Rolling and Automation, Northeastern University, Shenyang 110819, China

Received 1 April 2020; accepted 12 December 2020

Abstract: To electrochemically extract Pb from PbO at room temperature, a new electrolyte, urea–1-ethyl-3-methylimidazolium fluoride (urea–[EMIM]F), was synthesized to dissolve PbO. Afterwards, the electrochemical behavior of Pb in this electrolyte was studied. The density, viscosity and conductivity of this electrolyte were investigated before electroextraction. The electrochemical behavior of Pb in the urea–[EMIM]F system was recorded via cyclic voltammograms, chronoamperometry and potentiostatic electrolysis. The results illustrate that Pb can be electrochemically extracted from PbO in this system at room temperature and that Pb reduction involves a quasireversible process and follows a one-step and two-electron transfer process. The reduction of Pb proceeds with a three-dimensional (3D) progressive model. With an increase in temperature, the onset potentials for Pb reduction shift anodically. The diffusion coefficient of Pb(II) is determined to be $6.88 \times 10^{-10} \text{ cm}^2/\text{s}$ at 353 K. Additionally, spherical Pb particles are obtained after electrodeposition in the urea–[EMIM]F system via potentiostatic electrolysis.

Key words: Pb; ionic liquids; imidazolium fluoride; electrodeposition; viscosity

1 Introduction

Lead is often used in lead–acid batteries that account for more than 85% of the global lead consumption [1]. Traditionally, lead is produced from galena through desulfurization (PbS to PbO) and deoxidation (PbO to Pb) in furnaces at a high temperature [2]. However, this process requires high energy consumption. Therefore, many laboratory studies have focused on hydro-metallurgical methods that are operated at room temperature in aqueous systems, such as alkaline, nitrate, iodide, bromide, acetate, and methane-sulfonate.

Room-temperature ionic liquids (RTILs) are considered alternative electrolytes in laboratory studies during metal electrodeposition [3–5]. KATAYAMA et al [6] electrochemically extracted lead from Pb(TFSA)₂ in a BMPTFSA system at 298 K. BHATT et al [7] electrodeposited lead from Pb(NO₃)₂ and Pb(CO₃)₂ in the DIMCARB system. WANG et al [8] reported Pb electroreduction from PbCl₂ in the MBIC–AlCl₃ system. Similarly, TSAI et al [9] studied Pb electrodeposition in EMIBF₄ using PbCl₂ as the lead source. Furthermore, SIMONS et al [10] studied the extraction of metallic lead in a [C₂mim][NTf₂] system containing 50 mmol of Pb(NTf₂)₂.

In the above studies, lead salts were used as

lead sources. It is interesting to use lead oxide as a lead source during metal electrodeposition [2,11]. However, it is difficult to dissolve metal oxides in molecular solvents, except for acids and bases [12]. Therefore, specific solvents have been developed by researchers. Previously, ABBOTT et al [13] reported that PbO_2 has a high solubility (9.157 mg/mL) in urea–choline chloride (ChCl). In addition, YANG and REDDY [14] presented the concentration of PbO (7.5×10^{-3} mol/L) and the voltammetric behavior of lead in the urea–ChCl system. RU et al [15–17] electrochemically analyzed various morphologies of lead from PbO –urea–ChCl and discussed the mechanism of PbO electroreduction in an ethylene glycol–ChCl system. HE et al [18] investigated the voltammetric and chronoamperometric behavior of PbO in urea–EMIC system. Moreover, LIAO et al [19] and YE H et al [20,21] electrochemically studied the recovery of lead from PbO in urea–ChCl and in [Hbet][TFSA], respectively. Recently, LI and LI [22] have extracted Pb from PbO in acetamide-1-methylimidazolium trifluoromethylsulfonate in a low-temperature system at room temperature. LIU et al [23] reported that Co–Nd films were electro-synthesized from a urea–ChCl system. CVETKOVIĆ et al [24] electrodeposited Al metal from an AlCl_3 –urea RTIL. ALESARY et al [25] electrodeposited Zn–Sn alloys and studied the corrosion behavior of Zn–Sn coatings from the ChCl system. These unexpected solvating attributes are attractive in the processing of metal oxides and open a new route for metal electrodeposition from metal oxide precursors at room temperature.

However, compared with common EMIM salts, [EMIM]F can provide an interesting RTIL in a solvated form for metal electrodeposition. Lead electrodeposition in a urea–1-ethyl-3-methylimidazolium chloride (urea–[EMIM]Cl) system has been reported in our previous work [18]. To avoid chlorine generation at the anode, we developed urea–[EMIM]F as an electrolyte instead of urea–[EMIM]Cl in this study. In addition, urea–[EMIM]Cl is sensitive to air, and lead electrodeposition in this system is required to be conducted in an inert-atmosphere glove box, while urea–[EMIM]F is stable in air. Additionally, urea–[EMIM]F has a higher conductivity than urea–[EMIM]Cl. Although [EMIM]F has been reported by HAGIWARA et al [26,27], RIJKSEN

and ROGERS [28], ZHU et al [29] and by our group [30–32], to the best of our knowledge, the application of [EMIM]F in lead extraction has not been elucidated so far. These findings expanded the range of applications of [EMIM]F and provided a simple route to extract lead particles from precursors of metal oxides at room temperature. Based on this study, the urea–[EMIM]F system was capable of dissolving PbO and extracting lead. The density, viscosity and conductivity of urea–[EMIM]F were determined, and the electrochemical characteristics of lead were investigated via cyclic voltammograms, chronoamperometry and potentiostatic electrolysis.

2 Experimental

2.1 Chemicals and materials

1-ethyl-3-methylimidazolium chloride, that is, [EMIM]Cl (>98%, Lanzhou Institute of Chemical Physics, China) was purified according to the procedure described in literatures [30,32,33]. Before use, the urea (99%, Sinopharm Chemical Reagent Co., Ltd., China) was dried in a vacuum for 10 h at 393 K. AgF (>98%, Alfa Aesar) and PbO (99.99%, Sinopharm Chemical Reagent Co., Ltd., China) were used as-received. Tungsten foils (99.99%, 0.3 mm thick) were used as the substrate for electrodeposition [18].

[EMIM]F was synthesized according to the procedure described in previous studies [30,32,33]. 25 mL of 2.76 mol/L [EMIM]Cl aqueous solution and 20 mL of 3.45 mol/L AgF aqueous solution were mixed and stirred for 24 h. A white precipitate was produced and centrifuged. The supernatant was dried for 48 h in a vacuum and [EMIM]F was obtained. Two samples of [EMIM]F were titrated via AgNO_3 and NaCl , respectively. No precipitates suggested that Cl^- and Ag^+ were removed completely. The water content in [EMIM]F was measured to be 16.97% by Karl–Fischer titration. Additionally, urea and [EMIM]F were mixed at a molar ratio of 2:1 and the mixture was used to dissolve 1.4 mmol of PbO [18]. This final mixture was the labeled urea–[EMIM]F– PbO (0.31 mol/L).

2.2 Physical properties of urea–[EMIM]F

Measurements of the physical properties of urea–[EMIM]F were all performed according to literatures [30,34]. The densities of urea–[EMIM]F

(molar ratio 2:1) were examined by the Archimedean method at temperatures ranging from 333 to 373 K, the viscosities were measured via the rotation method on a viscometer (DV-2TLV, Brookfield), and conductivity measurements were completed using the impedance method.

2.3 Electrodeposition of lead

The lead extraction and electrochemical investigation in the urea-[EMIM]F-PbO system were completed according to procedures reported in literature [18]. Specifically, the electrochemical behavior was investigated by means of cyclic voltammograms and chronoamperometry techniques using an AUTOLAB (Metrohm PGSTAT 30, Switzerland) potentiostat/galvanostat controlled by the GPES software. The cyclic voltammograms and chronoamperometric experiments were performed in a three-electrode cell, which consisted of a tungsten wire (0.11 cm², 99.95%) as the working electrode (WE), a platinum wire (0.055 cm², 99.95%) as the counter electrode (CE) and a silver wire (0.055 cm², 99.95%) as the quasi-reference electrode (QRE). All electrodes were polished with emery paper, degreased with an anhydrous alcohol solution in an ultrasonic bath, washed with doubly distilled water, and air-dried before conducting the experiments.

Electrodeposition experiments were conducted on a tungsten (W) substrate (0.55 cm², 99.99%) in a three-electrode cell. The lead electrodeposition was performed at -0.62 V (vs Ag) and 353 K on the W substrate via potentiostatic electrolysis. After electrodeposition was completed, the substrate was immersed in an anhydrous alcohol solution to remove the electrolyte adhered to the surface. The phase constitutions of electrodeposits were detected via an X-ray diffractometer (XRD, PANalytical MPDDY 2094, Netherlands), and the elemental compositions and surface morphologies of the electrodeposits were examined using a scanning electron microscope (SEM, ZEISS ULTRA-43-13, Germany) equipped with an energy-dispersive spectroscope (EDS, X-Max 50, Oxford, England).

3 Results and discussion

3.1 Physical properties

Figure 1 shows the densities of urea-[EMIM]F (molar ratio 2:1) at different temperatures.

A linear decrease with increasing temperature was identified. A linear correlation was obtained using Eq. (1), which is similar to that of other imidazolium-based RTILs reported in literature [32] and indicates that the density of urea-[EMIM]F changes linearly with increasing temperatures from 333 to 373 K.

$$\rho = 1.4060 - 6.1133 \times 10^{-4} T \quad (1)$$

where ρ is the density in g/cm³ and T is the thermodynamic temperature in K.

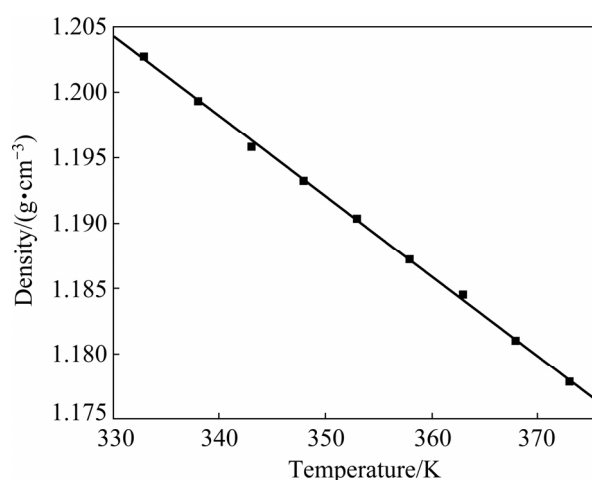


Fig. 1 Density of urea-[EMIM]F (molar ratio 2:1) as function of temperature

Figure 2 shows the viscosities for urea-[EMIM]F (molar ratio 2:1). These viscosities decrease with increasing temperature, which may be related to changes in van der Waals forces [35]. The viscosities do not decrease linearly with the increase of temperature. Similar behaviors were found in imidazole-based RTILs [36].

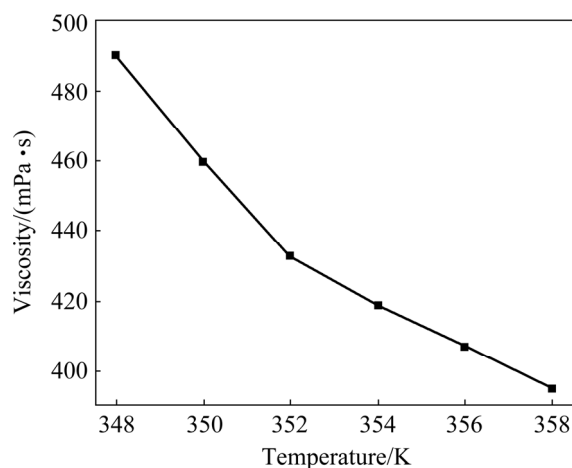


Fig. 2 Viscosity of urea-[EMIM]F (molar ratio 2:1) as function of temperature

Figure 3 shows the conductivity for urea-[EMIM]F and urea-[EMIM]Cl (molar ratio 2:1). Urea-[EMIM]F has conductivity varying from 6.59 to 24.52 mS/cm at temperatures between 333 and 373 K, which is higher than that of urea-[EMIM]Cl. This difference may be related to the ionic mobility being enhanced at a high temperature [37].

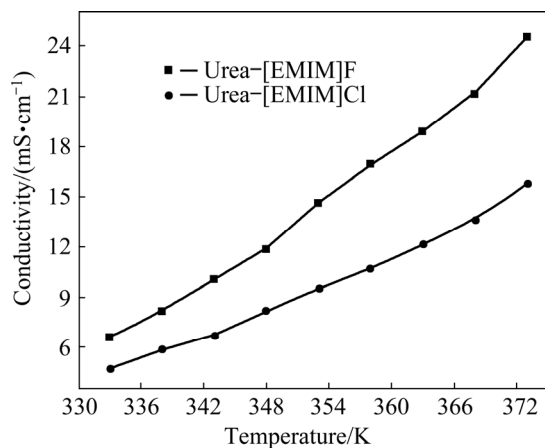


Fig. 3 Conductivity of urea-[EMIM]F and urea-[EMIM]Cl (molar ratio 2:1) as function of temperature

3.2 Cyclic voltammetry

To investigate the electrochemical behavior of lead in the urea-[EMIM]F (molar ratio 2:1) system, a linear scan voltammogram for urea-[EMIM]F (molar ratio 2:1) without lead was recorded from 0.56 to -0.8 V using a tungsten working electrode under a scan rate of 40 mV/s, which was considered a blank experiment, as shown in Fig. 4. There was no significant current within the electrochemical window, indicating that urea-[EMIM]F was electrochemically stable within the potential range. Figure 5 shows a cyclic voltammogram recorded from 0.25 to -0.65 V in urea-[EMIM]F (molar ratio 2:1) containing 0.31 mol/L PbO system under the same conditions. A cathodic peak at -0.476 V (vs Ag) and an anodic peak at -0.125 V were observed after the addition of PbO into urea-[EMIM]F. The metallic lead was obtained after potentiostatic electrolysis, as verified by XRD and EDS spectra. Therefore, the peak at -0.476 V was considered the electroreduction of Pb(II) to Pb. Similarly, the peak at -0.125 V corresponded to the dissolution of the reduced lead. These results indicate that the reduction of Pb(II) proceeds via a single-step and two-electron transfer process [2,18]. Figure 6 presents cyclic voltammograms for the urea-[EMIM]F-PbO (0.31 mol/L) system at

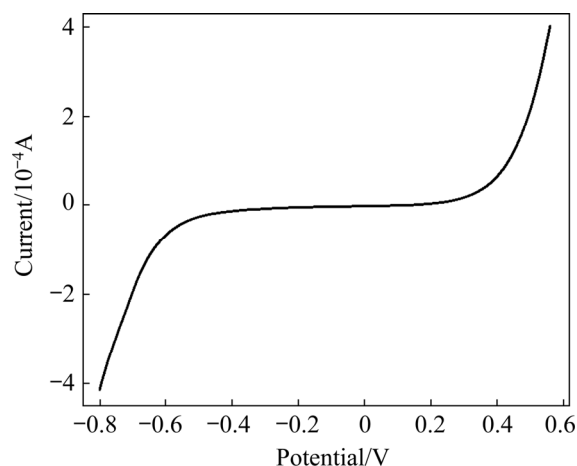


Fig. 4 Linear scan voltammogram of urea-[EMIM]F (molar ratio 2:1) (WE: W; $\nu=40$ mV/s; QRE: Ag; 353 K)

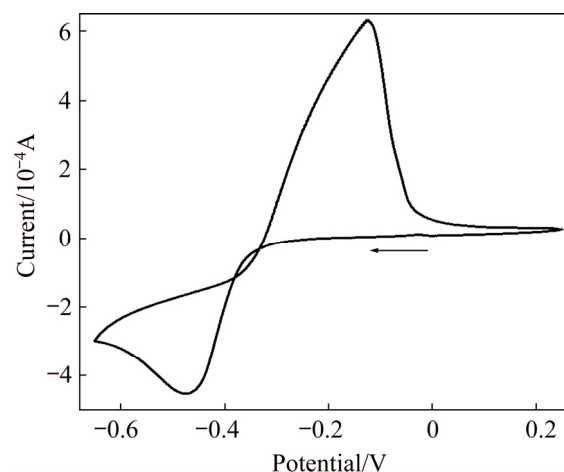


Fig. 5 Cyclic voltammogram for urea-[EMIM]F-PbO (0.31 mol/L) system (WE: W; $\nu=40$ mV/s; QRE: Ag; 353 K)

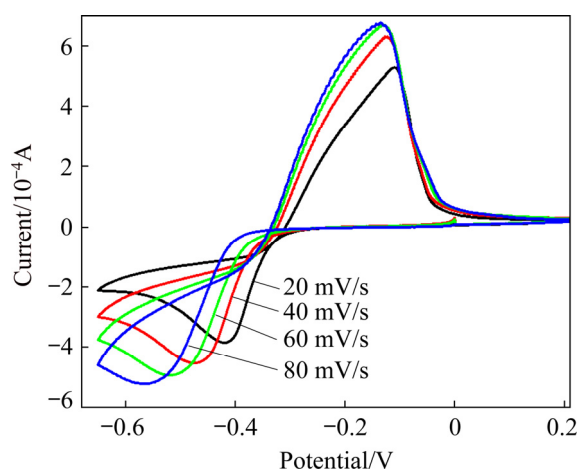


Fig. 6 Cyclic voltammograms for urea-[EMIM]F-PbO (0.31 mol/L) system at different scan rates (WE: W; QRE: Ag; 353 K)

different scan rates. The currents in the cathodic peaks (I_{pc}) and anodic peaks increased with increasing scan rates. The cathodic and anodic peak potentials shifted to increasingly negative values when the scan rate increased to higher values. The difference between the cathodic half-peak potential and the cathodic peak potential ($\varphi_{pc/2}-\varphi_{pc}$) increased as the scan rate increased, and exceeded the limit for a reversible process (33.5 mV, 353 K), as shown in Table 1. BABD and FAULKNER [38], and MATSUDA and AYABE [39] suggested that zone boundaries for reversible ($\Delta \geq 15$), quasireversible ($15 \geq \Delta \geq 10^{-2(1+\alpha)}$), and totally irreversible ($\Delta \leq 10^{-2(1+\alpha)}$) systems can be calculated from Eq. (2). For the urea-[EMIM]F-PbO (0.31 mol/L) system, the Δ (Δ , α) was calculated to be 5.0591 via Eq. (2) and α was calculated to be 0.3670 via Eq. (3). Based on the function of Δ (Δ , α) with Δ and α [38,39], the reduction of lead in the urea-[EMIM]F system could be considered a quasi-reversible process. Some nucleation loops were detected during the cathodic sweep, indicating that lead electrodeposition requires an overpotential to initiate nucleation [2].

$$\varphi_{pc/2}-\varphi_{pc}=\Delta(A, \alpha)[RT/(nF)] \quad (2)$$

$$|\varphi_{pc}-\varphi_{pc/2}|=1.857RT/(anF) \quad (3)$$

where $\varphi_{pc/2}$ is the cathodic half-peak potential in V, φ_{pc} is the cathodic peak potential in V, α is the transfer coefficient, Δ is a parameter, Δ is a parameter that varies with Δ and α , n is the number of exchanged electrons, F is the Faraday constant of 96485 C/mol and R is the molar gas constant of 8.314 J/(K·mol).

Table 1 Values of φ_{pc} , $\varphi_{pc/2}$, $\varphi_{pc/2}-\varphi_{pc}$ and I_{pc} at different scan rates

$v/$ ($\text{mV}\cdot\text{s}^{-1}$)	$\varphi_{pc}/$ mV	$\varphi_{pc/2}/$ mV	$(\varphi_{pc/2}-\varphi_{pc})/$ mV	$I_{pc}/$ 10^{-4} A
20	-418.55	-369.61	48.94	3.85
40	-476.07	-405.63	70.44	4.54
60	-515.75	-430.86	84.89	4.95
80	-565.34	-461.84	103.50	5.24

3.3 Chronoamperometry

Figure 7 presents the chronoamperometric curves of the lead nucleation/growth process in the urea-[EMIM]F-PbO (0.31 mol/L) system at various potentials. These potential values were

chosen based on the value that failed to cause nucleation/growth, and negatively increased with the same gradient until full nucleation/growth. Chronoamperometric experiments were performed at potentials of -0.38, -0.44, -0.50, -0.54, -0.58 and -0.62 V. At the beginning of the experiment, each transient had a large decaying current due to the charge of the double-layer on the surface of the electrode. After dropping to a minimum value, these currents reversed and increased because of the nucleation of lead. The current in this stage is referred to as the Faraday current, which obtains an inflection point at t_m , where t_m is the time at the maximum current I_m [40,41]. All instantaneous currents decay after time t_m . As the potentials negatively increased, the I_m also increased, while t_m tended to decline. This may be attributed to less time to overlap with the discrete diffusion zone, and the enhancement of the nucleation rate and nucleation density at a higher cathodic potential [42].

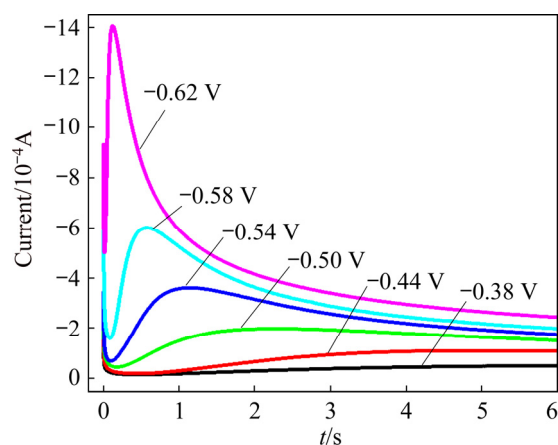


Fig. 7 Chronoamperometric curves for urea-[EMIM]F-PbO (0.31 mol/L) system (WE: W; QRE: Ag; 353 K) at different potentials

The instantaneous current relationship ($I-t^{-1/2}$) after t_m , which was obtained from Fig. 7 during the chronoamperometric experiments is shown in Fig. 8. A linear relationship with the characteristics of Cottrell behavior was discovered. Hence, the lead nucleation/growth in this system may follow a diffusion-controlled process [38].

The instantaneous model (Eq. (4)) and the progressive model (Eq. (5)) are often involved in metal electrodeposition [40,41]. For instantaneous model, the fixed nucleation sites on the electrode surface are all activated after each potential step,

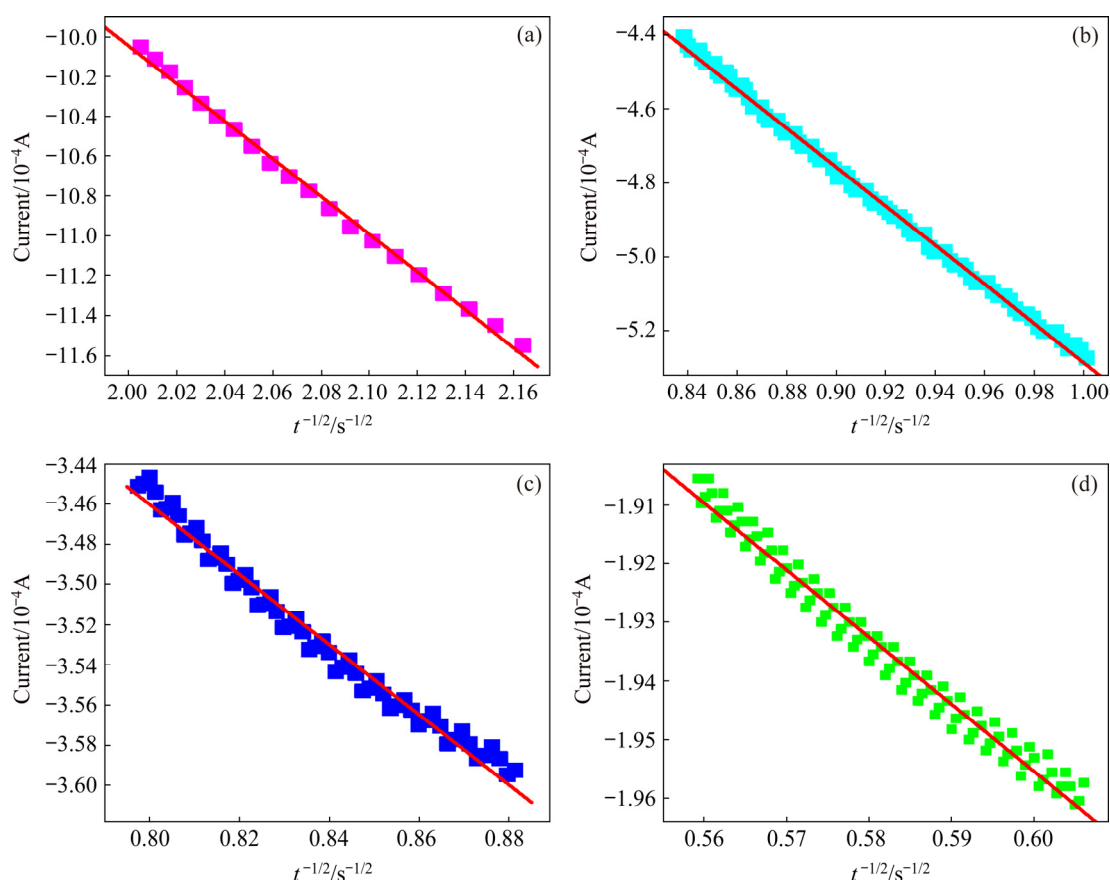


Fig. 8 Correlations between current and time ($t^{-1/2}$) in chronoamperometric experiments at different potentials: (a) $\varphi=-0.62$ V; (b) $\varphi=-0.58$ V; (c) $\varphi=-0.54$ V; (d) $\varphi=-0.50$ V

and the number of nucleation sites is constant during the chronoamperometric experiment. However, the nucleation sites are gradually activated and increase as time increases in the progressive model. To identify the mode of lead nucleation, the experimental data in Fig. 7 are normalized by I/I_m versus t/t_m and then compared with Eqs. (4) and (5). The results agree well with the 3D progressive model (Fig. 9). Over a longer period, the experimental data are larger than the theoretical data, which may be related to partial kinetic control during electrodeposition [2,43,44]. Therefore, electrodeposition could be considered a 3D progressive process.

Instantaneous model:

$$\left(\frac{I}{I_m}\right)^2 = 1.9542 \left(\frac{t_m}{t}\right) \left\{ 1 - \exp \left[-1.2564 \left(\frac{t}{t_m}\right) \right] \right\}^2 \quad (4)$$

Progressive model:

$$\left(\frac{I}{I_m}\right)^2 = 1.2254 \left(\frac{t_m}{t}\right) \left\{ 1 - \exp \left[-2.3367 \left(\frac{t}{t_m}\right)^2 \right] \right\}^2 \quad (5)$$

where I is the instantaneous current in A, and t is the instantaneous time in s.

3.4 Effect of temperature

Figure 10 shows that the cathodic peak potentials and the onset potentials anodically shift as the temperature rises. In addition, the current of the reduction and oxidation peaks also increases significantly. These are related to the enhanced diffusion of species at high temperatures. Chronoamperometric curves of the urea-[EMIM]F-PbO (0.31 mol/L) system at different temperatures are shown in Fig. 11. The current reaches a maximum in a shorter time as the temperature increases due to the nucleation/growth of lead nuclei at a faster rate. The corresponding Cottrell plots in the inset of Fig. 11 show the change in slopes with temperature, illustrating that lead diffusion is easier at high temperatures. The diffusion coefficient can be determined by Eq. (6) [40,41]:

$$I_m^2 t_m = 0.2598 D F^2 n^2 c_0^2 \quad (6)$$

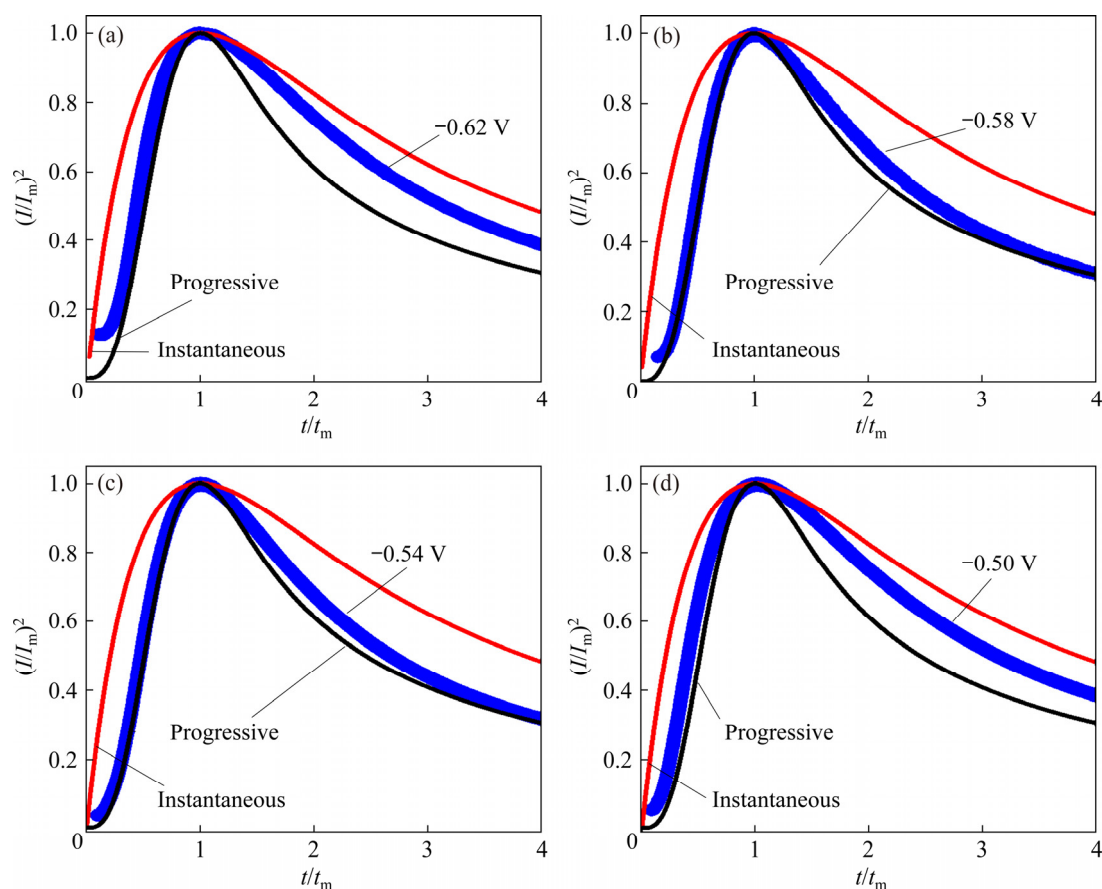


Fig. 9 Comparison between experimental curves for urea-[EMIM]F-PbO (0.31 mol/L) system and theoretical models of instantaneous and progressive nucleation at different potentials: (a) -0.62 V; (b) -0.58 V; (c) -0.54 V; (d) -0.50 V

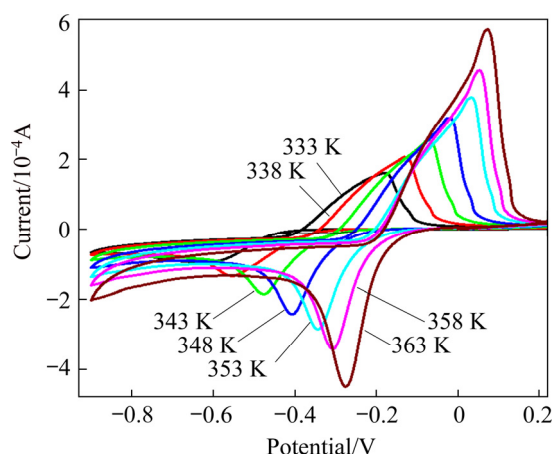


Fig. 10 Cyclic voltammograms for urea-[EMIM]F-PbO (0.31 mol/L) at different temperatures (WE: W; ν : 40 mV/s; QRE: Ag)

where D is the diffusion coefficient in cm^2/s , F is the Faraday constant of 96485 C/mol, n is the number of exchanged electrons, and c_0 is the metal ion bulk concentration in mol/mL. The values of I_m and t_m can be obtained from Fig. 11. The lead diffusion coefficients of substituting values for n ,

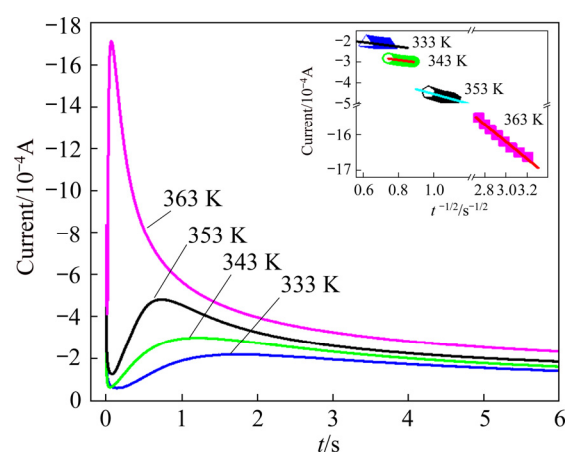


Fig. 11 Chronoamperometric curves for urea-[EMIM]F-PbO (0.31 mol/L) system at different temperatures (Cathodic potential: -0.58 V; Inset: corresponding Cottrell plots (WE: W; QRE: Ag))

F and c_0 into Eq. (6) are listed in Table 2. In addition, Table 3 presents the lead diffusion coefficients obtained from different RTILs. The small difference may be related to various ionic liquids and different temperatures.

Table 2 Lead diffusion coefficients (D) for urea–[EMIM]F–PbO system at various temperatures

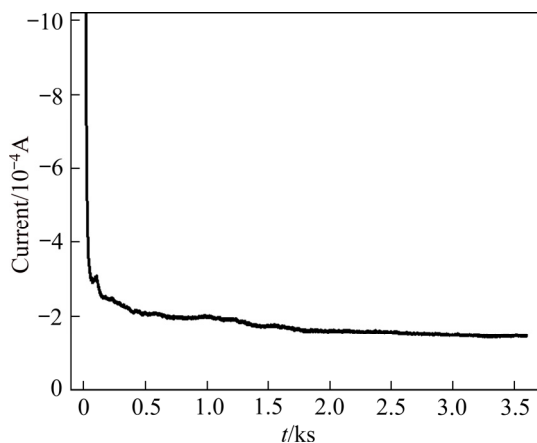
Temperature/K	$D/(\text{cm}^2 \cdot \text{s}^{-1})$
333	3.20×10^{-10}
343	4.44×10^{-10}
353	6.88×10^{-10}
363	8.09×10^{-10}

Table 3 Diffusion coefficients of Pb(II) in different ionic liquids

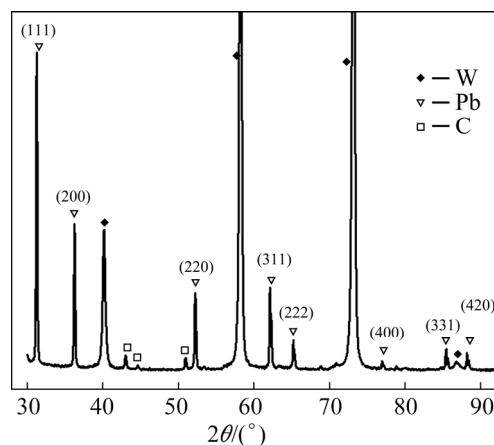
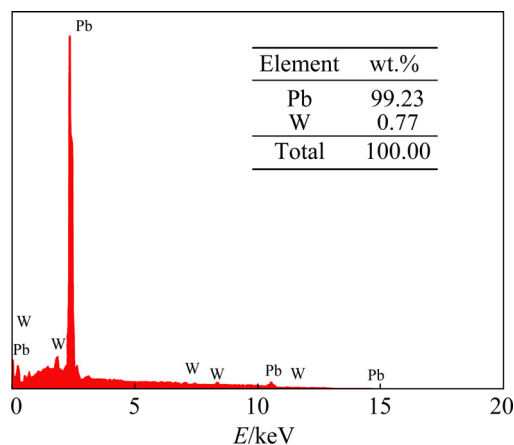
Ionic liquid	T/K	$D/(\text{cm}^2 \cdot \text{s}^{-1})$	Ref.
Urea–[EMIM]F	353	6.88×10^{-10}	This work
Urea–EMIC	353	1.67×10^{-8}	[18]
MIMTfO	373	3.60×10^{-8}	[45]
Urea–ChCl	363	2.20×10^{-7}	[19]
Urea–BMIC	353	3.22×10^{-8}	[2]

3.5 Electrodeposition and characterization

Potentiostatic electrolysis was completed on a tungsten substrate. During electrodeposition, the electrolyte was not stirred. Figure 12 presents the variation in current during potentiostatic electrolysis in urea–[EMIM]F–PbO (0.31 mol/L) system at -0.62 V (vs Ag) and 353 K for 60 min. The current decreases rapidly at the beginning and then remains relatively stable over the rest of the experimental period. After potentiostatic electrolysis, electrodeposits are obtained on the tungsten substrate and characterized by XRD, EDS and SEM.

**Fig. 12** Current–time curve recorded during potentiostatic electrodeposition of Pb in urea–[EMIM]F–PbO (0.31 mol/L) system (Substrate: W; Cathodic potential: -0.62 V; T : 353 K)

The XRD pattern of electrodeposits is shown in Fig. 13. 2θ angles (31.3° , 36.3° , 52.2° , 62.1° , 65.2° , 85.4° , 88.2°) are associated with lead (ICCD files No. 03-065-2873), while the remaining peaks correspond to the tungsten substrate and carbon from electrolyte decomposition. No peaks of lead oxide are discovered in this XRD pattern, suggesting that Pb(II) in urea–[EMIM]F was electroreduced to Pb. Figure 14 shows the EDS analysis results of the electrodeposits. The peaks in this spectrum are related to lead and tungsten substances. Figure 15 shows the morphologies of the electrodeposits. Uniform and spherical lead particles were observed with sizes of about 100 nm, which were evenly distributed on the tungsten substrate. Similar morphologies were also discovered by LIU et al [2] for the urea–BMIC system.

**Fig. 13** XRD pattern of electrodeposits obtained from urea–[EMIM]F–PbO (0.31 mol/L) system (Substrate: W; Cathodic potential: -0.62 V; T : 353 K)**Fig. 14** EDS spectrum of electrodeposits obtained from urea–[EMIM]F–PbO (0.31 mol/L) system (Substrate: W; Cathodic potential: -0.62 V; T : 353 K)

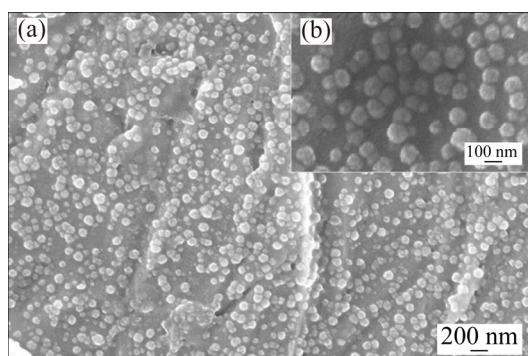


Fig. 15 Lower (a) and higher (b) magnification SEM images of electrodeposits obtained from urea–[EMIM]F–PbO (0.31 mol/L) system (Substrate: W; Cathodic potential: -0.62 V; T : 353 K)

4 Conclusions

(1) Urea–[EMIM]F is capable of dissolving PbO. The lead particles were then electrochemically extracted from urea–[EMIM]F–PbO (0.31 mol/L) system at room temperature.

(2) The density, viscosity and conductivity of urea–[EMIM]F were recorded. The density linearly decreased and the conductivity increased as the temperature increased from 333 to 373 K. The viscosity decreased with increasing temperature.

(3) The reduction of Pb(II) involves a quasi-reversible, one-step and two-electron transfer process. The lead electrodeposition follows a 3D progressive nucleation and a growth model governed by diffusion mixing. The diffusion coefficient of Pb(II) in urea–[EMIM]F was determined to be 6.88×10^{-10} cm²/s at 353 K, and increased with increasing temperature.

(4) Uniform spherical lead particles were electrochemically extracted from the urea–[EMIM]F–PbO (0.31 mol/L) system at room temperature via potentiostatic electrolysis, as verified by XRD, EDS and SEM.

Acknowledgments

The authors are grateful for the financial supports from the National Natural Science Foundation of China (51804070, 52074084) and Fundamental Research Funds for the Central Universities of China (N172502003).

References

[1] TAN S, PAYNE D J, HALLETT J P, KELSALL G H.

Developments in electrochemical processes for recycling lead–acid batteries [J]. *Current Opinion in Electrochemistry*, 2019, 16: 83–89.

- [2] LIU A M, SHI Z N, REDDY R G. Electrodeposition of Pb from PbO in urea and 1-butyl-3-methylimidazolium chloride deep eutectic solutions [J]. *Electrochimica Acta*, 2017, 251: 176–186.
- [3] LIU Ai-min, GUO Meng-xia, LÜ Zi-yang, ZHANG Bao-guo, LIU Feng-guo, TAO Wen-ju, YANG You-jian, HU Xian-wei, WANG Zhao-wen, LIU Yu-bao, SHI Zhong-ning. Electrochemical behavior of tantalum in ethylene carbonate and aluminum chloride solvate ionic liquid [J]. *Transactions of Nonferrous Metals Society of China*, 2020, 30(8): 2283–2292.
- [4] DEVI N. Solvent extraction and separation of copper from base metals using bifunctional ionic liquid from sulfate medium [J]. *Transactions of Nonferrous Metals Society of China*, 2016, 26(3): 874–881.
- [5] GONG Kai, HUA Yi-xin, XU Cun-ying, ZHANG Qi-bo, YAN Li, RU Juan-jian, JIE Yan-fei. Electrodeposition behavior of bright nickel in air and water-stable betaine·HCl–ethylene glycol ionic liquid [J]. *Transactions of Nonferrous Metals Society of China*, 2015, 25(7): 2458–2465.
- [6] KATAYAMA Y, FUKUI R, MIURA T. Electrodeposition of lead from 1-butyl-1-methylpyrrolidinium bis (trifluoromethylsulfonyl) amide ionic liquid [J]. *Journal of the Electrochemical Society*, 2013, 160(6): D251–D255.
- [7] BHATT A I, BOND A M, ZHANG J. Electrodeposition of lead on glassy carbon and mercury film electrodes from a distillable room temperature ionic liquid, DIMCARB [J]. *Journal of Solid State Electrochemistry*, 2007, 11(12): 1593–1603.
- [8] WANG Feng-xia, PAN Ge-bo, LIU Ying-dan, XIAO Yan. Pb deposition onto Au(111) from acidic chloroaluminate ionic liquid [J]. *Chemical Physics Letters*, 2010, 488(4–6): 112–115.
- [9] TSAI R W, HSIEH Y T, CHEN P Y, SUN I W. Voltammetric study and electrodeposition of tellurium, lead, and lead telluride in room-temperature ionic liquid 1-ethyl-3-methylimidazolium tetrafluoroborate [J]. *Electrochimica Acta*, 2014, 137: 49–56.
- [10] SIMONS T J, PEARSON A K, PAS S J, MACFARLANE D R. The electrochemical cycling and electrodeposition of lead from 1-ethyl-3-methylimidazolium bis (trifluoromethanesulfonyl) imide ionic liquid [J]. *Electrochimica Acta*, 2015, 174: 712–720.
- [11] ZHANG Bao-guo, YAO Yu, SHI Zhong-ning, XU Jun-li, WANG Zhao-wen. Direct electrochemical deposition of lithium from lithium oxide in a highly stable aluminium-containing solvate ionic liquid [J]. *Chem Electro Chem*, 2018, 5(22): 3368–3372.
- [12] ABBOTT A P, CAPPER G, DAVIES D L, SHIKOTRA P. Processing metal oxides using ionic liquids [J]. *Mineral Processing and Extractive Metallurgy*, 2006, 115(1): 15–18.
- [13] ABBOTT A P, CAPPER G, DAVIES D L, MCKENZIE K J, OBI S U. Solubility of metal oxides in deep eutectic solvents based on choline chloride [J]. *Journal of Chemical & Engineering Data*, 2006, 51(4): 1280–1282.

- [14] YANG H X, REDDY R G. Fundamental studies on electrochemical deposition of lead from lead oxide in 2:1 urea/choline chloride ionic liquids [J]. *Journal of the Electrochemical Society*, 2014, 161(10): D586–D592.
- [15] RU Juan-jian, HUA Yi-xin, XU Cun-ying, LI Jian, LI Yan, WANG Ding, QI Can-can, JIE Yan-fei. Morphology-controlled preparation of lead powders by electrodeposition from different PbO-containing choline chloride–urea deep eutectic solvent [J]. *Applied Surface Science*, 2015, 335: 153–159.
- [16] RU Juan-jian, HUA Yi-xin, XU Cun-ying, LI Jian, LI Yan, WANG Ding, QI Can-can, GONG Kai. Electrochemistry of Pb(II)/Pb during preparation of lead wires from PbO in choline chloride–urea deep eutectic solvent [J]. *Russian Journal of Electrochemistry*, 2015, 51(8): 773–781.
- [17] RU Juan-jian, WANG Ding, XU Cun-ying, LI Jian, LI Yan, ZHOU Zhong-ren, GONG Kai. Mechanistic insight of in situ electrochemical reduction of solid PbO to lead in ChCl–EG deep eutectic solvent [J]. *Electrochimica Acta*, 2015, 186: 455–464.
- [18] HE Wen-cai, LIU Ai-min, GUAN Jin-zhao, SHI Zhong-ning, GAO Bing-liang, HU Xian-wei, WANG Zhao-wen. Pb electrodeposition from PbO in the urea/1-ethyl-3-methylimidazolium chloride at room temperature [J]. *RSC Advances*, 2017, 7(12): 6902–6910.
- [19] LIAO Y S, CHEN P Y, SUN I W. Electrochemical study and recovery of Pb using 1:2 choline chloride/urea deep eutectic solvent: A variety of Pb species PbSO₄, PbO₂, and PbO exhibits the analogous thermodynamic behavior [J]. *Electrochimica Acta*, 2016, 214: 265–275.
- [20] YEH H W, TANG Y H, CHEN P Y. Electrochemical study and extraction of Pb metal from Pb oxides and Pb sulfate using hydrophobic Brønsted acidic amide-type ionic liquid: A feasibility demonstration [J]. *Journal of Electroanalytical Chemistry*, 2018, 811: 68–77.
- [21] YEH H W, CHANG C J, HUANG G G, CHEN P Y. Electrochemical conversion of ionic liquid–lead sulfate paste into metallic lead or lead (IV) oxide: Extracting lead from water-insoluble lead salt and formation of cobalt oxide electrocatalyst via galvanic displacement [J]. *Journal of Electroanalytical Chemistry*, 2019, 834: 64–70.
- [22] LI Min, LI Ying. Direct electrochemical reduction of solid lead oxide in acetamide-1-methylimidazolium trifluoromethylsulfonate low-temperature molten salt [J]. *JOM*, 2020, 72: 3806–3811.
- [23] LIU A M, SHI Z N, REDDY R G. Electrochemical synthesis of Co–Nd films in urea and choline chloride deep eutectic solvents [J]. *Metallurgical and Materials Transactions B*, 2020, 51(3): 1162–1168.
- [24] CVETKOVIĆ V, VUKIĆEVIĆ M, JOVIĆEVIĆ N, STEVANOVIĆ S, JOVIĆEVIĆ J. Aluminum electrodeposition under novel conditions from AlCl₃–urea deep eutectic solvent at room temperature [J]. *Transactions of Nonferrous Metals Society of China*, 2020, 30(3): 823–834.
- [25] ALESARY H, ISMAILX H, SHILTAGH M, ALATTAR R, AHMED L, WATKINS M, RYDER K. Effects of additives on the electrodeposition of ZnSn alloys from choline chloride/ethylene glycol-based deep eutectic solvent [J]. *Journal of Electroanalytical Chemistry*, 2020, 874: 114517.
- [26] HAGIWARA R, HIRASHIGE T, TSUDA T, ITO Y. A highly conductive room temperature molten fluoride: EMIF·2.3 HF [J]. *Journal of the Electrochemical Society*, 2002, 149(1): D1–D6.
- [27] HAGIWARA R, HIRASHIGE T, TSUDA T, ITO Y. Acidic 1-ethyl-3-methylimidazolium fluoride: A new room temperature ionic liquid [J]. *Journal of Fluorine Chemistry*, 1999, 99(1): 1–3.
- [28] RIJKSEN C, ROGERS R D. A solventless route to 1-ethyl-3-methylimidazolium fluoride hydrofluoride, [C₂mim][F]·xHF [J]. *The Journal of Organic Chemistry*, 2008, 73(14): 5582–5584.
- [29] ZHU Zhi-qiang, JIANG Ming-yue, ZHENG Chang-ge, XIAO Ji-chang. Efficient synthesis of 1-alkyl-3-methylimidazolium fluorides and possibility of the existence of hydrogen bonding between fluoride anion and C (sp³)–H [J]. *Journal of Fluorine Chemistry*, 2012, 133 : 160–162.
- [30] WANG De-xi, ZHONG Xiong-wei, LIU Feng-guo, SHI Zhong-ning. Electrodeposition of aluminum from AlCl₃-1-ethyl-3-methylimidazolium fluoride [J]. *International Journal of Electrochemical Science*, 2019, 14: 9482–9489.
- [31] LIU Feng-guo, ZHONG Xiong-wei, XU Jun-li, WANG Zhao-wen, SHI Zhong-ning. Facile synthesis and characterization of 1-ethyl-3-methylimidazolium fluoride ionic liquid [J]. *Journal of Physics: Conference Series*, 2019, 1347: 012109.
- [32] LIU Feng-guo, ZHONG Xiong-wei, XU Jun-li, KAMALI A, SHI Zhong-ning. Temperature dependence on density, viscosity, and electrical conductivity of ionic liquid 1-ethyl-3-methylimidazolium fluoride [J]. *Applied Sciences*, 2018, 8(3): 356.
- [33] HE Wen-cai, CHEN Peng, DENG Wen-tao, SHI Zhong-ning, GAO Bing-liang, HU Xian-wei, XU Jun-li, WANG Zhao-wen. Electrosynthesis of Cu₅Zn₈ alloy in zinc oxide–urea/1-ethyl-3-methylimidazolium fluoride system at 353 K [J]. *International Journal of Electrochemical Science*, 2017, 12: 1521–1534.
- [34] LIU Cheng-yuan, CHEN Wen-ting, WU Zi-mo, GAO Bing-liang, HU Xian-wei, SHI Zhong-ning, WANG Zhao-wen. Density, viscosity and electrical conductivity of AlCl₃–amide ionic liquid analogues [J]. *Journal of Molecular Liquids*, 2017, 247: 57–63.
- [35] ZHANG Q H, VIGIER K D O, ROYER S, JEROME F. Deep eutectic solvents: Syntheses, properties and applications [J]. *Chemical Society Reviews*, 2012, 41(21): 7108–7146.
- [36] AKIHIRO N, HAYAMIZU K, WATANABE M. Pulsed-gradient spin-echo ¹H and ¹⁹F NMR ionic diffusion coefficient, viscosity, and ionic conductivity of non-chloroaluminate room-temperature ionic liquids [J]. *The Journal of Physical Chemistry B*, 2001, 105(20): 4603–4610.
- [37] ABBOTT A P, BOOTHBY D, CAPPER G, DAVIES D L, RASHEED R K. Deep eutectic solvents formed between choline chloride and carboxylic acids: versatile alternatives to ionic liquids [J]. *Journal of the American Chemical Society*, 2004, 126(29): 9142–9147.
- [38] BARD A J, FAULKNER L R. *Electrochemical methods:*

- Fundamentals and applications [M]. 2nd ed. New York: John Wiley & Sons, 2001: 228–239.
- [39] MATSUDA H, AYABE Y. On the theory of Randles–Sevcik cathode ray polarography [J]. Journal for Electrochemistry, Reports of the Bunsen Society for Physical Chemistry, 1955, 59(6): 494–503.
- [40] SCHARIFKER B, HILLS G. Theoretical and experimental studies of multiple nucleation [J]. Electrochimica Acta, 1983, 28(7): 879–889.
- [41] GUNAWARDENA G, HILLS G, MONTENEGRO I, SCHARIFKER B. Electrochemical nucleation: Part I. General considerations [J]. Journal of Electroanalytical Chemistry and Interfacial Electrochemistry, 1982, 138(2): 225–239.
- [42] PLETCHER D. A first course in electrode processes [M]. London: Royal Society of Chemistry, 2009: 154–187.
- [43] LANGEROCK S, HEERMAN L. Study of the electrodeposition of rhodium on polycrystalline gold electrodes by quartz microbalance and voltammetric techniques [J]. Journal of the Electrochemical Society, 2004, 151(3): C155–C160.
- [44] HE Ping, LIU Hong-tao, LI Zhi-ying, LI Jing-hong. Electrodeposition of platinum in room-temperature ionic liquids and electrocatalytic effect on electro-oxidation of methanol [J]. Journal of the Electrochemical Society, 2005, 152(4): E146–E153.
- [45] LI Min, LI Ying. Electrodeposition of lead from 1-methylimidazolium trifluoromethylsulfonate ionic liquid [J]. International Journal of Electrochemical Science, 2018, 13: 9759–9770.

含 PbO 的尿素-1-乙基-3-甲基氟化咪唑体系在 353 K 下电化学提取铅

何文才^{1,2}, 刘凤国¹, 钟熊伟³, 杨山², 石忠宁⁴

1. 东北大学 多金属共生矿生态化冶金教育部重点实验室, 沈阳 110819;
2. Department of Chemistry, Physics and Atmospheric Science, Jackson State University, Jackson, MS 39217, USA;
3. 清华大学 清华-伯克利深圳学院&清华深圳国际研究生院 深圳盖姆石墨烯中心, 深圳 518055;
4. 东北大学 轧制技术及连轧自动化国家重点实验室, 沈阳 110819

摘要: 为了能在室温下从氧化铅中电化学提取铅, 合成一种新的电解质尿素-1-乙基-3-甲基氟化咪唑(urea-[EMIM]F)以溶解氧化铅, 并研究铅在此电解质中的电化学行为。电化学提取前, 研究该电解质的密度、黏度和电导率。采用循环伏安法、计时电流法和恒电位电解技术研究铅在尿素-1-乙基-3-甲基氟化咪唑中的电化学行为。结果表明: 采用该电解质可在室温下从氧化铅中电化学提取铅; 铅的还原遵循一步两电子的准可逆过程和三维(3D)连续成核模型; 随着温度的升高, 铅还原的起始电位逐渐向阳极移动; 在 353 K 下 Pb(II)的扩散系数为 $6.88 \times 10^{-10} \text{ cm}^2/\text{s}$; 对尿素-1-乙基-3-甲基氟化咪唑体系进行恒电位电沉积后, 获得球状铅颗粒。

关键词: 铅; 离子液体; 氟化咪唑; 电沉积; 黏度

(Edited by Wei-ping CHEN)